

## Articles

### A 3D-QSAR Study on the Structural Requirements for Binding to CB<sub>1</sub> and CB<sub>2</sub> Cannabinoid Receptors

Maria Fichera,<sup>\*,†</sup> Gabriele Cruciani,<sup>\*,‡</sup> Alfredo Bianchi,<sup>§</sup> and Giuseppe Musumarra<sup>†</sup>

Dipartimento di Chimica, Università di Catania, Viale A. Doria, 6, 95125 Catania, Italy; Dipartimento di Chimica, Università di Perugia, Via Elce di Sotto, 8, 06100 Perugia, Italy; Istituto di Farmacologia, Facoltà di Medicina, Università di Catania, Viale A. Doria, 6, 95125 Catania, Italy

Received May 6, 1999

A 3D-QSAR study was carried out on 20 cannabinoids for which the binding affinities ( $K_i$ ) with respect to CB<sub>1</sub> and CB<sub>2</sub> receptors, determined in the same cell line, were available. For the first time three series of significantly different chemical structures such as  $\Delta^9$ -THC analogues, anandamides, and indoles were included in a single 3D-QSAR model, to obtain information on the interactions of all ligands with both CB<sub>1</sub> and CB<sub>2</sub> receptors and on their receptor selectivity.  $\Delta^9$ -THC was chosen as the structural template for alignment. The 3D-structure–activity correlation obtained by the GOLPE procedure provided a partial least squares (PLS) model with a very good predictive ability for the CB<sub>1</sub> receptor affinity of all compounds. The model allowed us to identify seven different regions in the space that contribute to explain the above binding affinities. External validation of the interpretation of the 3D-QSAR model was derived from a response-independent procedure such as principal components analysis (PCA). The CB<sub>2</sub> receptor model evidenced, besides the seven regions found for the CB<sub>1</sub> receptor, a new characteristic region for the CB<sub>2</sub> receptor. Another PCA, using 10 GRID probes, provided further evidence of receptor selectivity regions. One region opposite to the amidic NH of CB<sub>1</sub> selective O585 appears to be responsible for the CB<sub>1</sub> selectivity, while an interaction region opposite to the carbonyl of CB<sub>2</sub> selective JWH-015 appears to be involved in the CB<sub>2</sub> binding selectivity.

#### Introduction

Indian hemp, *Cannabis sativa*, has long been used for both its psychotropic and pharmacological effects.  $\Delta^9$ -THC ( $\Delta^9$ -tetrahydrocannabinol), isolated and characterized in 1964,<sup>1</sup> was identified as the principal psychoactive component of marijuana.

$\Delta^9$ -THC belongs to a family of about 60 bi- and tricyclic compounds named cannabinoids. Most of these natural products have a 6,6'-dimethylpyrane ring (the B ring, which sometimes is present in an open form), a variously substituted aromatic ring (A ring), and a variously unsaturated cyclohexyl ring (C ring). They include nonpsychoactive cannabidiol and cannabinolic acid.

The structure elucidation of  $\Delta^9$ -THC allowed the design of synthetic strategies: in 1986 over 300 compounds, reviewed by Razdan,<sup>2</sup> were already available for studying their pharmacological properties and the structural features required for their biological activity. A wide range of pharmacological effects was described for  $\Delta^9$ -THC:<sup>3</sup> analgesic, antiemetic, antiinflammatory, bronchodilatory, and anticonvulsant effects already known for cannabis preparations, as well as reduction of blood ocular pressure in glaucomic patients and

alleviation of neurological disorders in multiple sclerosis and Huntington's chorea.

The pharmacological activity of cannabinoids is mediated by two recently identified cannabinoid receptors, CB<sub>1</sub><sup>4</sup> and CB<sub>2</sub><sup>5</sup>. The CB<sub>1</sub> receptor is localized in specific brain areas<sup>6,7</sup> (cerebral cortex, hippocampus, basal ganglia, cerebellum), while the peripheral receptor CB<sub>2</sub> is localized in the spleen, monocytes, macrophages and lymphocytes,<sup>6,7</sup> so it appears to be involved in antiinflammatory and immunosuppressive activities. Both the central and the peripheral cannabinoid receptors belong to the seven trans-membrane (7TM) spanning receptor family and contain the domains necessary for coupling to G-proteins.

In 1992 anandamide was identified as an endogenous ligand for cannabinoid receptors<sup>8</sup> and was shown to share with  $\Delta^9$ -THC and other cannabinoids most pharmacological and biochemical properties. The discovery of endogenous ligands prompted further studies aimed at the elucidation of the chemical, pharmacological, and pharmacodynamic behavior of CB<sub>1</sub> and CB<sub>2</sub> receptors and of cannabinoid and cannabinomimetic ligands. These studies pointed out that, in addition to classical cannabinoids, other structurally different molecules may interact with the same receptors, inducing analogous responses. At present, cannabinoid agonists can be classified into at least four groups: classic cannabinoids, bicyclic cannabinoids, aminoalkylindoles, and anandamide analogues.<sup>9</sup>

\* To whom correspondence should be addressed. Tel: +39 095 334 175. Fax: +39 095 580 138. E-mail: gmusumarra@dipchi.unict.it.

<sup>†</sup> Dipartimento di Chimica.

<sup>‡</sup> Università di Perugia.

<sup>§</sup> Istituto di Farmacologia, Università di Catania.

Traditional SAR studies on cannabinoids indicated the structural requirements for the biological activity of  $\Delta^9$ -THC and its analogues: (1) the free phenolic hydroxyl group;<sup>10</sup> (2) the extension and branching of the pentyl side chain responsible for the greatly increased affinity of the dimethylheptyl (DMH) derivative;<sup>2,11</sup> and (3) the orientation and the chemical nature of the C<sub>9</sub> substituent.<sup>12,13</sup> Reggio et al.<sup>14</sup> also described a region of steric interaction, located near the top of the carbocyclic ring in the bottom face of the molecule, that is a region occupied by atoms in inactive analogues and not occupied by atoms in active analogues.

Further SAR studies suggested that anandamide and its analogues, although belonging to a class of compounds different than bi- and tricyclic cannabinoids, do contain specific structural features necessary for binding to CB<sub>1</sub> cannabinoid receptor and for biological activity.<sup>15–18</sup>

Thomas et al.,<sup>19</sup> employing molecular dynamics, selected a pharmacophoric conformation of anandamide and predicted its potency by a quantitative model of cannabinoid structure–activity relationships based only on classical and nonclassical cannabinoids.<sup>20</sup>

Recently, a different conformation of anandamide, exhibiting a different alignment of pharmacophoric groups with respect to those of  $\Delta^9$ -THC, was reported.<sup>21</sup> Also in this case the potency of anandamide was predicted from a 3D-QSAR model obtained using CoMFA for a training set of 29 classical and nonclassical cannabinoid analogues.

All 3D-QSAR studies reported so far are based on analogue structures and consider only the CB<sub>1</sub> receptor.<sup>20–23</sup> To our knowledge, no 3D-QSAR model is available for the CB<sub>2</sub> receptor or for the binding of structurally different ligands to the CB<sub>1</sub> receptor. Since the three-dimensional structure of cannabinoid receptors is still unknown and little knowledge is available on the nature of the ligand–receptor interaction, this work is aimed to study by 3D-QSAR a set of molecules belonging to structurally different series, including noncyclic compounds such as anandamide and its derivatives. To obtain general structural information about the CB<sub>1</sub> and CB<sub>2</sub> receptors and to derive a model able to predict the potency of compounds not included in the data set as well as their selectivity, receptor affinity was chosen as the dependent variable. Indeed, SAR studies already revealed a high degree of correlation between receptor affinity and pharmacological potency, which implies the involvement of these receptors in most behavioral effects of cannabinoids.<sup>24–26</sup>

The modeled molecules were selected from literature data<sup>27</sup> reporting the binding affinities ( $K_i$ ) with respect to CB<sub>1</sub> and CB<sub>2</sub> receptors for three series of significantly different structures: (i) THC and derivatives, (ii) anandamide and derivatives, and (iii) indole derivatives or azoles. The selected set of molecules, exhibiting a wide variation of both structure and activity, appears to be suitable for the present investigation due to the homogeneity of the biological response, as all the binding affinities were determined in the same cell line. Table 1 reports the structures of compounds **1–20**, belonging to all three series, and their CB<sub>1</sub> and CB<sub>2</sub> receptor affinities, expressed as  $\log K_i$ .

## Methods

**Molecular Structures and Energy Minimization.** The structures of all molecules were generated using the Sybyl 6.4 molecular modeling package<sup>28</sup> and their energies were minimized using the Powell method with a conjugated gradient of 0.05 kcal/Å convergent criterion provided by the Tripos force field. All molecules were considered in their neutral form without taking into account electrostatic interactions.

The structure of  $\Delta^9$ -THC was built in agreement with the structure of  $\Delta^9$ -tetrahydrocannabinolic acid B as determined by X-ray crystallography.<sup>29</sup> THC analogues were modeled by modifying this basic structure. In molecules showing rotational freedom (especially bicyclic cannabinoids), rotatable bonds were sampled in order to determine minimum energy conformations.

An initial structure of anandamide was generated from the molecular fragments provided within Sybyl for arachidonic acid and ethanolamine. The conformation of anandamide, due to its extreme mobility, was minimized by constraining the appropriate pharmacophore atoms to maintain the distance found for the corresponding atoms in  $\Delta^9$ -THC, according to the conformation proposed by Thomas et al.<sup>19</sup> In particular, the distance between the carbamido and the hydroxyl oxygens in anandamide was assumed to be equal to that between the pyran and the phenolic oxygens in  $\Delta^9$ -THC (4.8 Å), the distance between the carbamido oxygen and the terminal linear chain carbon (C<sub>20</sub>) in anandamide was assumed to be equal to that between the pyran oxygen and the terminal alkyl chain carbon in  $\Delta^9$ -THC (9.33 Å), the distance between the hydroxyl oxygen and C<sub>20</sub> in anandamide was assumed to be equal to that between the phenolic oxygen and the terminal alkyl chain carbon in  $\Delta^9$ -THC (9.27 Å), and the distance between the C<sub>5</sub> ethylenic arachidonyl carbon of anandamide and the hydroxyl oxygen was assumed to be equal to that between the C<sub>7</sub> ring carbon and the phenolic oxygen in  $\Delta^9$ -THC (5.24 Å). Finally, the molecule was energy minimized with no constraints and a looped conformation was obtained.

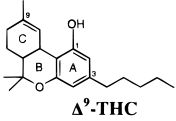
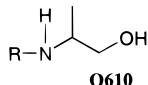
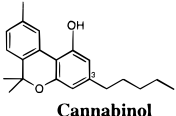
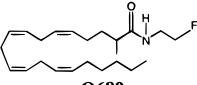
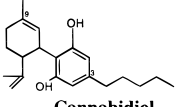
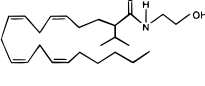
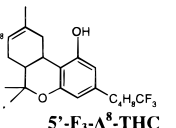
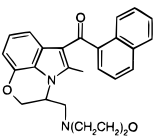
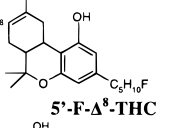
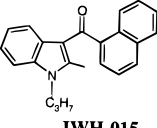
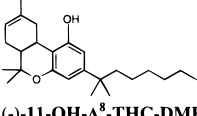
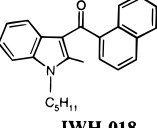
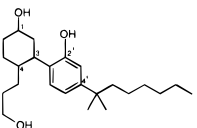
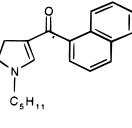
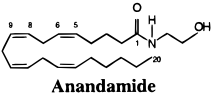
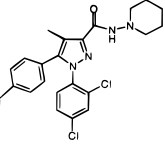
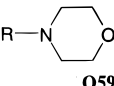
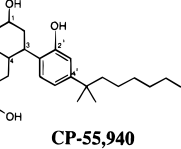
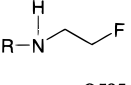
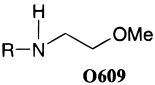
Anandamide analogues were modeled by modifying this basic structure. Energy minimization on fully constrained molecules was followed by further minimization after removing constraints. Aminoalkylindoles and azoles were subjected to conformational analysis using the systematic search methodology. The torsion angle window for systematic conformational perturbation was 30° and a few different low-energy conformations were selected for all molecules to be superimposed to  $\Delta^9$ -THC.

**Alignment of the Molecules.**  $\Delta^9$ -THC was chosen as the structural template for the alignment process. THC analogues possessing the aromatic ring and the aliphatic side chain were aligned to  $\Delta^9$ -THC by superimposing the above common groups, while for indole derivatives different alignments were considered. In particular, the indole ring nitrogen was aligned with the  $\Delta^9$ -THC C<sub>3</sub> aromatic carbon where the side chain is attached, the N-linked chain was aligned with the  $\Delta^9$ -THC side chain, the naphthalene moiety was superimposed to the  $\Delta^9$ -THC nonaromatic carbocyclic C ring (with different orientation from perpendicular to skewed with respect to the above ring), and finally the 3-keto group was aligned with the  $\Delta^9$ -THC hydroxyl group or, alternatively, with the pyran oxygen, depending on steric hindrance. The pyrazole antagonist **19** exhibits a peculiar alignment due to the presence of the amido carbonyl and of the piperidine and N-2 pyrazole nitrogens. The alignments with respect to  $\Delta^9$ -THC of typical derivatives **8**, **16**, **18**, and **19** are shown in stereoview in Figure 1.

For anandamide and its analogues, the alignment was performed as suggested by Thomas et al.<sup>19</sup> by superposing the carboxamide oxygen with the pyran oxygen in  $\Delta^9$ -THC, the hydroxyl group of ethanol with the phenolic hydroxyl group, the five terminal carbons with the pentyl side chain, and the polyolefin loop with the cannabinoid tricyclic ring.

**Molecular Description: GRID Force Field.** The GRID program<sup>30–32</sup> was used to describe the previously superposed molecular structures. GRID is a computational procedure for detecting energetically favorable binding sites of molecules.

**Table 1.** Receptor Affinities of Modeled Molecules<sup>a</sup>

No.	log K <sub>i</sub> CB <sub>1</sub> (nM)	log K <sub>i</sub> CB <sub>2</sub> (nM)	No.	log K <sub>i</sub> CB <sub>1</sub> (nM)	log K <sub>i</sub> CB <sub>2</sub> (nM)
1	1.60	1.56	12 <sup>c</sup>	2.14	2.60
					
<b>Δ<sup>9</sup>-THC</b>			<b>O610</b>		
2	2.49	1.98	13	0.76	2.12
					
<b>Cannabinol</b>			<b>O689</b>		
3	3.64	3.46	14	3.60	3.71
					
<b>Cannabidiol</b>			<b>O694</b>		
4	1.3	1.48	15	0.28	-0.55
					
<b>5'-F<sub>3</sub>-Δ<sup>8</sup>-THC</b>			<b>WIN-55,212-2</b>		
5	1.76	0.94	16	2.58	1.14
					
<b>5'-F-Δ<sup>8</sup>-THC</b>			<b>JWH-015</b>		
6	-0.14	-0.66	17	0.98	0.47
					
<b>(-)-11-OH-Δ<sup>8</sup>-THC-DMH</b>			<b>JWH-018</b>		
7 <sup>b</sup>	1.79	1.37	18	1.94	2.50
					
<b>CP-56,667</b>			<b>JWH-030</b>		
8	1.95	2.57	19	1.09	2.85
					
<b>Anandamide</b>			<b>SR-141716A</b>		
9 <sup>c</sup>	3.06	2.73	20 <sup>d</sup>	-0.19	-0.007
					
<b>O595</b>			<b>CP-55,940</b>		
10 <sup>c</sup>	0.93	2.51			
					
<b>O585</b>					
11 <sup>c</sup>	3.26	2.65			
					
<b>O609</b>					

<sup>a</sup> Data from ref 27. <sup>b</sup> (1*S*,3*S*,4*S*)-3-[2'-Hydroxy-4'-(1,1-dimethylheptyl)-phenyl]-4-(3-hydroxypropyl)cyclohexan-1-ol. <sup>c</sup> R = Arachidonyl. <sup>d</sup> (1*R*,3*R*,4*R*)-3-[2'-Hydroxy-4'-(1,1-dimethylheptyl)phenyl]-4-(3-hydroxypropyl)cyclohexan-1-ol.

The program calculates the interactions between the molecule and a probe group which is moved through a regular grid of points in a region of interest around the target molecule, and at each point, the interaction energy between the probe and the target molecule is calculated as the sum of Lennard-Jones ( $E_{LJ}$ ), hydrogen bond ( $E_{HB}$ ), and electrostatic interactions ( $E_{EL}$ ):

$$E_{x,y,z} = \sum_{i=1}^N E_{LJ} + \sum_{i=1}^N E_{HB} + \sum_{i=1}^N E_{EL}$$

GRID contains a table of parameters to describe each type of atom occurring in each of the ligand molecules. These parameters define the strength of the Lennard-Jones, hydro-

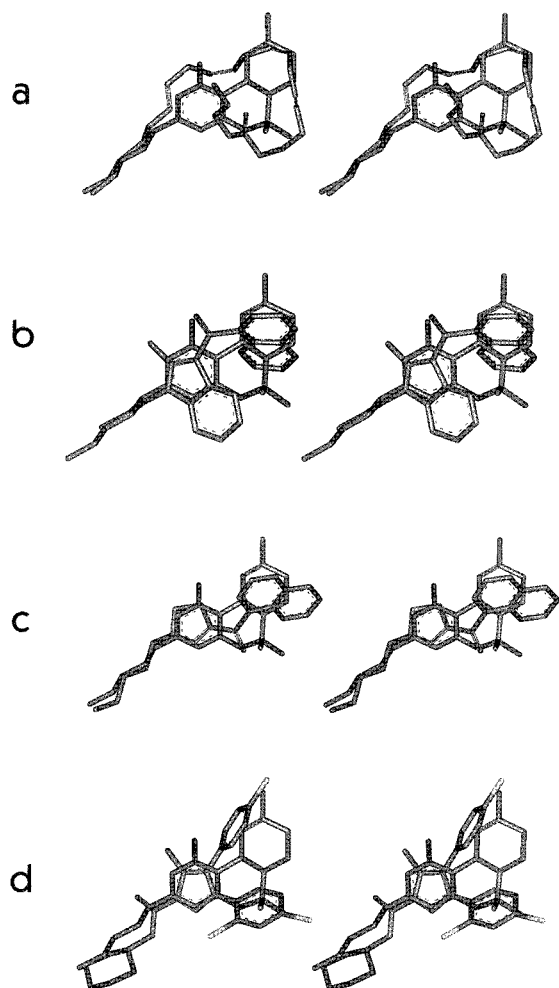


**Figure 1.** Alignment of  $\Delta^9$ -THC **1** with anandamide **8** (a), with JWH-015 **16** (b), with JWH-30 **18**, and with the antagonist **19** (d).

gen bond, and electrostatic interactions made by an atom and are used in order to evaluate the energy functions. GRID probes are very specific. They give precise spatial information, and their specificity and sensitivity are an advantage since the probes may be representative of the important chemical groups present in the active site, provided that the statistical method used for the analysis can distinguish between different types of interactions.

A CB<sub>1</sub> pseudoreceptor model reported in the literature<sup>22</sup> suggests that aspartic acid and histidine residues are involved in the interactions with cannabinoids. Therefore, in the present work, for both CB<sub>1</sub> and CB<sub>2</sub> receptors, the multiatom carboxy anion (COO<sup>-</sup>) was chosen to mimic the aspartic acid probe. GRID analysis using the N-sp<sup>2</sup> probe, typical of histidine, showed no significant differences with those using carboxylate. In the selectivity study, different probes were used: O (sp<sup>2</sup> carbonyl oxygen), O- (sp<sup>2</sup> phenolate oxygen), O= (O of sulfate/sulfonamide), O: (sp<sup>2</sup> carboxy oxygen atom), OH (sp<sup>2</sup> hydroxy group), O1 (sp<sup>3</sup> hydroxy group), N1: (sp<sup>3</sup> NH with lone pair), N1+ (sp<sup>3</sup> amine NH cation), N3+ (NH<sub>3</sub><sup>+</sup> amine cation), and DRY (a hydrophobic probe).

The energy calculations were performed using 1.0 Å spacing between the grid points. Each set of calculated interaction energies contained in the resulting three-dimensional matrix, arranged as a one-dimensional vector, was used as input for the program GOLPE.<sup>33</sup>

**QSAR Analysis.** The GRID variables matrix for the COO<sup>-</sup> probe was correlated with the CB<sub>1</sub> receptor affinities by a PLS model using the GOLPE procedure.

To obtain a model with better predictive capability, variable selection was operated by zeroing values with absolute values

smaller than 0.06 kcal/mol and removing variables with standard deviation below 0.1. In addition, variables which exhibited only two values and had a skewed distribution were also removed in order to avoid their high leverage, so that a set of 4346 variables was eventually used from the original 17 550 grid variables.

The smart region definition (SRD) algorithm<sup>34</sup> was applied on this matrix with the following parameters: (a) 410 seeds (10% active variables) selected in the PLS weights space, (b) critical distance cutoff of 2.5 Å, and (c) collapsing distance cutoff of 4 Å. The regions found (390) were used in a fractional factorial design (FFD)<sup>33,35</sup> variable selection procedure, using a leave-one-out (LOO) cross-validation methodology. The model dimensionality chosen was that showing the best predictive ability, and the active variables remaining after applying the FFD variable selection procedure<sup>33-35</sup> were 1295. Finally, new PLS and PCA models were derived only on the basis of the active variables/regions.

The PLS model for the CB<sub>2</sub> receptor was obtained on the set of the selected 20 molecules maintaining the same conformation of all molecules. Again, variable selection was performed on the same 4346 variables and the SRD algorithm was applied with the same parameters; 1556 active variables were obtained. A new PLS model based only on these active variables/regions was finally carried out.

## Results and Discussion

The present work represents the first attempt to include three different structural classes of compounds in a single 3D-QSAR model for CB<sub>1</sub> and CB<sub>2</sub> receptors with the aim to obtain wider general information on the interactions of ligands with both receptors and on their selectivity.

The examined classes of compounds are structurally very different. Cannabinoids represent a class of bicyclic (nonclassical cannabinoids) or tricyclic (classical cannabinoids) compounds showing at least an aromatic ring and a side chain attached to the C<sub>3</sub> carbon of the aromatic ring. Other rings may be aromatic or nonaromatic and variously substituted. In general, cannabinoids are rigid molecules which can be easily superimposed. On the other hand, anandamide and its analogues are very flexible molecules which can assume both linear and nonlinear conformations, although biologically active molecules rarely assume linear conformations.

Aminoalkylindoles and azoles studied in the present work (**15-17**) possess a 3-keto naphthyl substituent and include the 3-substituted monocyclic *N*-alkyl derivative (**18**). Finally the pyrazole derivative SR-141716A (**19**), an antagonist to the CB<sub>1</sub> receptor, was also included in the model.

The choice to include three different classes of compounds in the same model implies difficulties in the selection of the right conformation and in the alignment of the molecules to a template.  $\Delta^9$ -THC was chosen as template because of a wider availability of biological, pharmacological, and structural data.

The alignment of cannabinoids to  $\Delta^9$ -THC was straightforward by superimposing common groups. For anandamide, the conformation proposed by Thomas et al.<sup>19</sup> was adopted, because a looped conformation of anandamide is energetically favorable and a structural correlation between this structure and classical cannabinoids can be obtained by superimposing the features described in a previous section. In fact, in this conformation, electronegative regions associated with the hydroxyl and carbonyl oxygen can be superimposed

**Table 2.** Fitting and Prediction Capabilities of CB<sub>1</sub> and CB<sub>2</sub> Receptor Models Obtained by GOLPE Variable Selection

PLS components	CB <sub>1</sub> receptor model		CB <sub>2</sub> receptor model	
	$R^2$	$Q^2$	$R^2$	$Q^2$
1	0.94	0.81	0.95	0.66
2	0.98	0.85	0.98	0.78
3	0.99	0.84	0.99	0.78

to similar electronegative regions in  $\Delta^9$ -THC, as well as the linear carbon side chain and  $\pi$ -electron rich regions can be superimposed to the corresponding regions in  $\Delta^9$ -THC. Moreover, the proposed conformation of anandamide is supported by previous conformational studies on arachidonic acid, indicating the ability of the acid to form packed structures<sup>36</sup> as well as by evidence that arachidonic acid adopts a similar conformation during self-epoxidation reactions.<sup>37</sup>

Following the above criterion of alignment, the pyran ring was considered in the matching scheme, although it does not appear to be responsible for biological activity, as it can be eliminated or its oxygen can be replaced by a carbon or a nitrogen without significant loss of potency.<sup>38–40</sup> Nevertheless, the pyran ring appears to be important for the structural and electronic alignment, regardless of its contribution to the overall binding activity. The suitability of the selected alignment criterion, however, will be confirmed by evaluating the prediction ability of the resulting models.

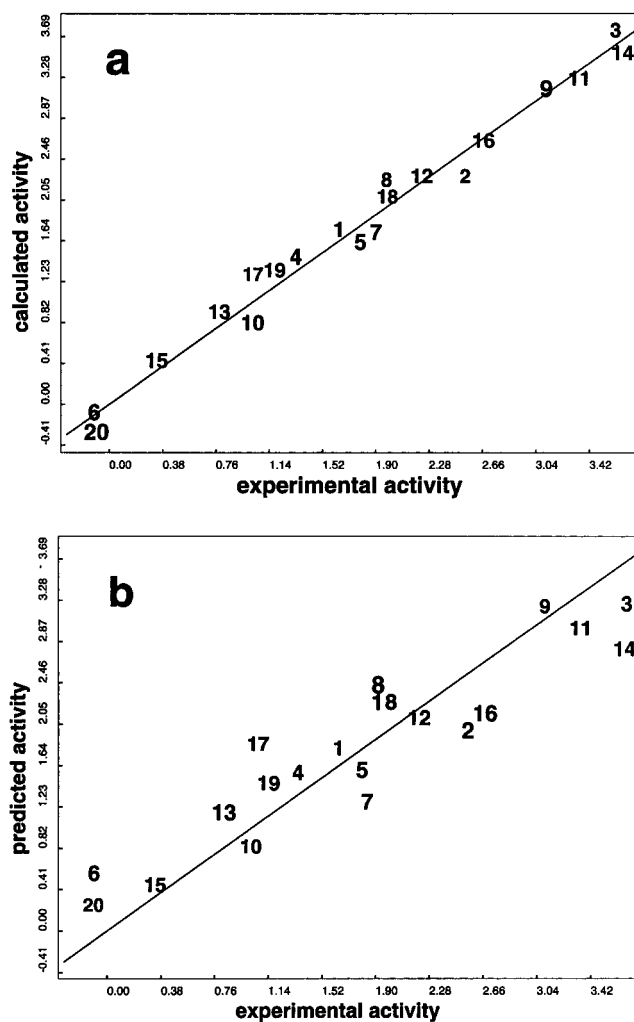
General guidelines for the alignment of derivatives **15–18** were already reported in the Methods section. However, it is worth mentioning here that the carbonyl oxygen was aligned with the phenolic oxygen of  $\Delta^9$ -THC for **16** and **17**, while for **15** and **18** the selected active conformations involved alignment with the  $\Delta^9$ -THC pyran oxygen. Each of the above alignments was the only one consistent with a satisfactory statistical model.

**CB<sub>1</sub> Receptor Model.** The structure–activity correlation was obtained by using the GOLPE procedure. The GOLPE analysis, using the SRD algorithm and the FFD variable selection procedure, identified the significant GRID variables corresponding to the regions of the molecules involved in the binding to the CB<sub>1</sub> receptor. The PLS model, derived on the 1295 variables selected from the starting 17 550, is optimal with only two PLS components.

As shown in Table 2, the first PLS component already explains 94% of variance in the CB<sub>1</sub> receptor binding affinity and is highly predictive ( $Q^2 = 0.81$ ). The second PLS component still improves both the fitting and the predictive abilities of the model, while the third PLS component has no further predictivity improvement. Therefore, the model's optimal dimensionality is given by two PLS components. Parts a and b of Figure 2 report, respectively, a graphical representation of the model fitting and prediction abilities.

The model is therefore successful in explaining a set of 20 molecules belonging to completely different structural classes, with a good prediction ability. Hence, it provides, for the first time, safe grounds for a unique pharmacophoric interpretation of the regions responsible for the CB<sub>1</sub> receptor affinity of all compounds.

Because satisfactory statistical parameters were achieved with only two PLS components, a very effective modeling and variable selection procedure was adopted.

**Figure 2.** (a) Experimental vs calculated inhibition constant ( $\log K_i$ ) from the CB<sub>1</sub> receptor model; (b) experimental vs predicted inhibition constant ( $\log K_i$ ) from the CB<sub>1</sub> receptor model.

In addition, the interpretation is much easier with respect to that of previously reported PLS models based only on homogeneous series of bicyclic and tricyclic derivatives, requiring up to eight PLS components to achieve a model<sup>21</sup> comparable in fitting ( $r_{\text{conv}}^2 = 0.992$ ) but much less effective in prediction ( $r_{\text{cv}}^2 = 0.598$ ).

The statistical significance and the sound interpretation of the CB<sub>1</sub> receptor model derived therefore provides strong evidence that the conformation of anandamide adopted by Thomas<sup>19</sup> and used in the present work is the most favorable one for interaction with cannabinoid receptors.

The GRID plot of the partial weights (Figure 3) identifies areas in space that contribute most to the CB<sub>1</sub> receptor binding affinity model. Figure 3 highlights seven areas representing the regions of interaction between the target molecules and the receptor and it includes, as an example, the structure of  $\Delta^9$ -THC. Light gray regions highlight areas where a polar group (e.g. an H bond donor in the ligand structure) causes an increase in the binding affinity, while dark gray regions highlight areas where interactions result in an overall binding affinity decrease. Conversely, an apolar group (e.g. a methyl in the ligand structure) interacting with

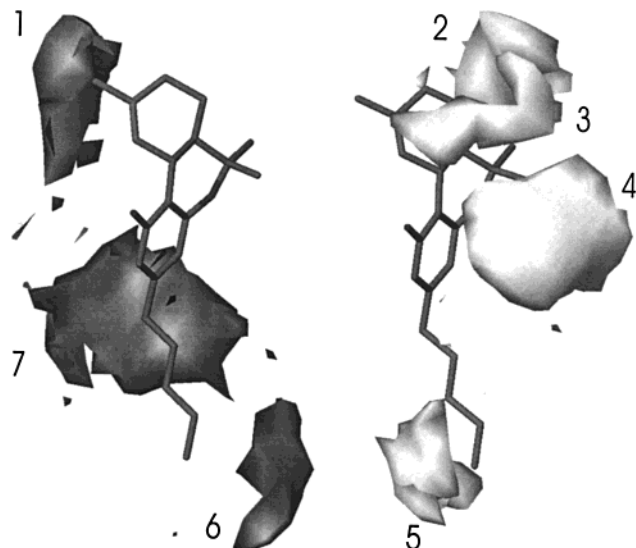


**Figure 3.** Grid plot of PLS partial weights for the CB<sub>1</sub> receptor model (see the text for discussion).

light gray or dark gray regions respectively causes a decrease or an increase in the binding affinity.

The methyl group attached to C<sub>9</sub> of  $\Delta^9$ -THC interacts with region 1 with a positive binding contribution. A bulky substituent at C<sub>9</sub> would protrude more deeply into the above interaction region with an expected activity increase.

The methyl groups at C<sub>6</sub> of  $\Delta^9$ -THC interact respectively with region 4 and with region 2, providing a negative contribution to the binding affinity. Therefore, removal of these methyls would favor binding to the CB<sub>1</sub> receptor while their substitution with polar groups (NH<sub>2</sub>, OH), giving a positive binding contribution, would result in a further affinity increase. Region 3 is very close to region 2 and exhibits the same characteristics.

The well-known high activity of 9-nor-9 $\beta$ -OH-hexahydrocannabinol (HHC),<sup>21,23</sup> where the C<sub>9</sub>-hydroxy substituent, if interacting with region 1, would produce a negative contribution for binding, could be due to the interaction of OH with region 3. The above interaction would, in that particular case, be possible due to the absence of the C<sub>9</sub>-C<sub>10</sub> double bond, which makes possible an arrangement of the OH group closer to region 3.

Interaction of the carbamido nitrogen of anandamide and derivatives with region 4 provides a relevant modulation of the binding affinities. The lack of the above interaction for derivatives **9**, **11**, and **14**, the conformation of which is such that the amido nitrogen lies away from region 4, results in a great affinity decrease (see Table 1).

Region 5 exhibits only a minor effect on the THC binding. Branching of the alkyl chain terminal carbons could decrease the binding affinity. Accordingly, the morpholine moiety of WIN-55,212 (**15**) interacting with region 5 contributes negatively to the CB<sub>1</sub> binding.

The presence of region 6 is consistent with the pharmacophoric relevance of the C<sub>3</sub> alkyl chain contributing positively to the CB<sub>1</sub> receptor binding. Extension of the five carbon chain by adding one or two carbons would favor the binding, while further extension would be detrimental to the binding due to steric hindrance.

The presence of region 7, where alkyl groups would improve the binding with the receptor, confirms literature data<sup>2,11</sup> that point out that branching at the first atom of the alkyl chain increases the binding affinity. Consistently, the highly active  $\Delta^9$ -THC derivative **6** exhibits both branching methyls (attached at C<sub>1</sub> of the linear chain) interacting with region 7 and a chain extension (7 carbon atoms) which is optimal for interaction with region 6.

The CB<sub>1</sub> affinities of indoles **15**–**17** depend mainly on favorable interactions of naphthyl and indole rings with regions 1 and 7, respectively; the above interactions are weaker for **16** and **17**. Compound **17**, however, benefits also from the interaction of a longer *N*-alkyl chain with region 6, resulting in affinity increase with respect to **16**.

The antagonist **19** exhibits favorable binding interactions of three chlorine atoms with regions 2, 3, and 4, respectively, as well as that of the piperidine ring with region 7.

The relative importance of the reported regions can be obtained from the numerical inspection and comparison of the partial weight PLS coefficients. Thus, regions 2, 4, and 7 are the most important for the binding affinity; therefore, changes in the groups interacting with the above regions are predicted to affect ligand affinity dramatically. Region 1 immediately follows in order of ranking, while regions 3, 5, and 6 are very similar to each other.

**Principal Component Analysis.** External validation to the interpretation of the 3D-QSAR PLS model for the CB<sub>1</sub> receptor might be derived from an independent procedure such as PCA on selected GRID variables.

Indeed, PCA extracts the most relevant statistical "factors" from a data matrix where a number of "objects" (i.e. 20 compounds) are characterized by a number of variables (i.e. 1295 GRID variables) without assuming any relationship with a "response" (in the present case the binding affinity). Therefore, the first and second principal components "scores" plot, opening a two-dimensional window into the multidimensional matrix space, will provide a very simple and "response unbiased" classification of the compounds. Inspection of the above plot may allow an interpretation of the significance of the factors responsible for compound classification based on GRID variables. The PCA score plot for compounds **1**–**20** is reported in Figure 4.

Figure 4 shows clearly that the first principal component (PC) score (*t*<sub>1</sub>) characterizes compounds **1**–**20** in order of decreasing binding affinities (i.e. activities), regardless of their structures (see also Table 1). Highly active compounds (e.g. **6**, **15**, and **20**) are located in the left part of the plot, while those with low activity (e.g. **3**, **9**, **11**, and **14**) are in the right part. This finding, achieved by a statistical method such as PCA, which ignores any "response" (i.e. binding or activity) data, provides strong evidence for the robustness of the model in selecting suitable GRID variables in relation to the CB<sub>1</sub> binding affinity. Moreover, the PC score plot contributes to classify compounds **1**–**20** according to their chemical structure.  $\Delta^9$ -THC derivatives are in fact in the lower region of the plot (i.e. they exhibit highly negative *t*<sub>2</sub> values), anandamides in the upright region

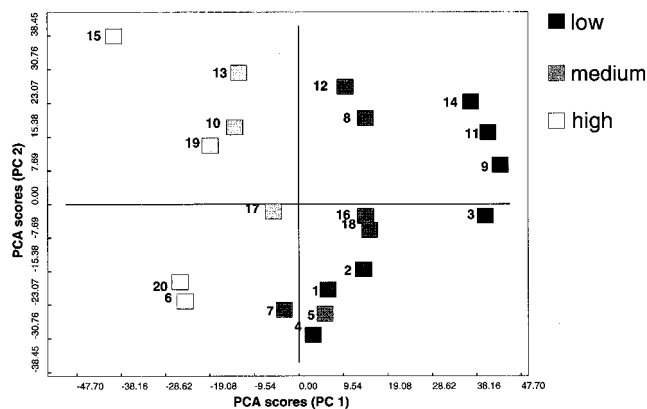


**Figure 4.** PCA score plot for compounds 1–20.  $t_1$  values characterize the compounds in order of decreasing affinity (Table 1). Compounds are colored according to their affinity value, i.e., light gray for high affinity compounds and dark gray for low affinity compounds.

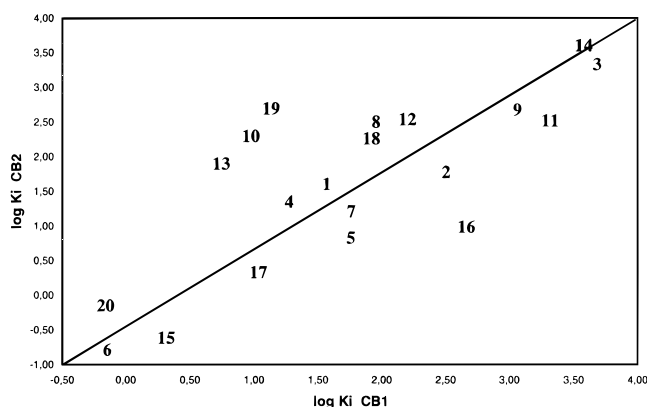


**Figure 5.** Plot of  $\log K_i$  for the  $CB_2$  receptor vs those for the  $CB_1$  receptor.

(i.e. exhibit positive  $t_2$  and  $t_1$  values), and indoles somewhat in middle.

**$CB_2$  Receptor Model.** The  $CB_1$  and  $CB_2$  receptors belong to the same family of receptors and exhibit 44% sequence homology, rising to 68% in the transmembrane domains,<sup>6,7</sup> an area thought to be involved in ligand recognition. As a consequence of this high degree of homology, it is not surprising that the binding affinities for  $CB_1$  and  $CB_2$  receptors are correlated. Figure 5, plotting the logarithms of the binding affinities for the  $CB_1$  receptor reported in Table 1 vs those for the  $CB_2$  receptor shows the correlation for compounds 1–20 ( $r^2 = 0.57$ ). Indeed, the correlation is highly significant ( $r^2 = 0.88$ ) with 16 compounds, when three compounds showing selectivity toward the  $CB_1$  receptor (10, 13 and 19) and the only  $CB_2$  selective one (16) are excluded. The above correlation is consistent with the hypothesis that all compounds keep the same conformation in both  $CB_1$  and  $CB_2$  receptor models.

In the case of the  $CB_2$  receptor model, the GOLPE procedure allowed selection of 1556 active variables starting from 17 550. A good PLS model derived on these active variables was achieved again with only two PLS components, as shown by the statistical parameters reported in Table 2. Parts a and b of Figure 6 report, respectively, a graphical representation of the  $CB_2$  model fitting and prediction abilities.

The GRID plot of the partial weights (Figure 7) allows

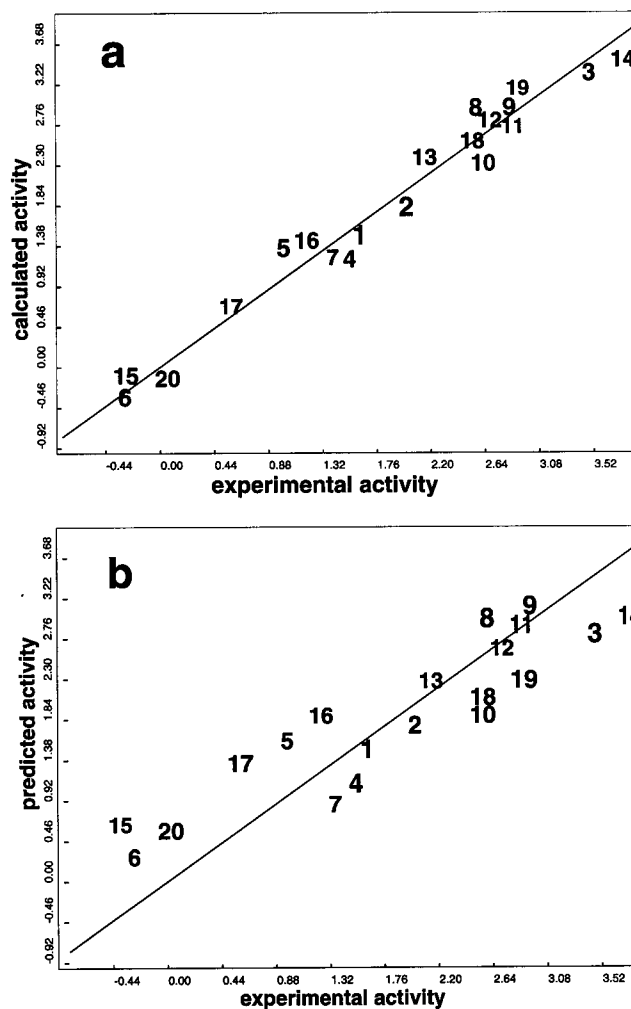


**Figure 6.** (a) Experimental vs calculated inhibition constant ( $\log K_i$ ) from the  $CB_2$  receptor model; (b) experimental vs predicted inhibition constant ( $\log K_i$ ) from the  $CB_2$  receptor model.

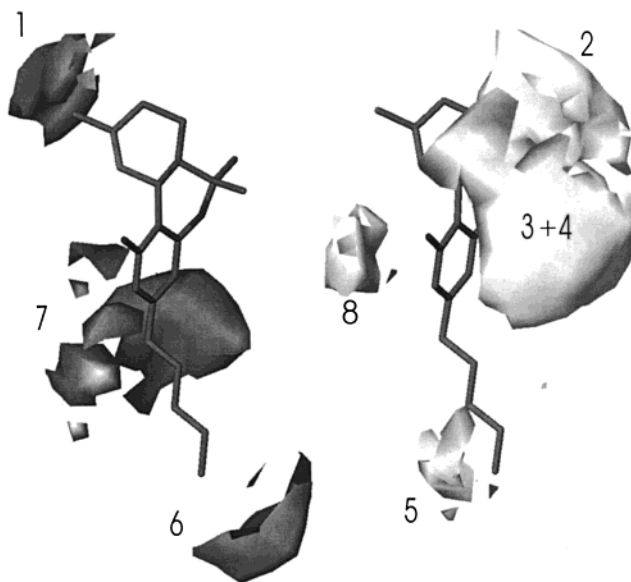


**Figure 7.** Grid plot of PLS partial weights for the  $CB_2$  receptor model (see text for discussion).

us to identify regions of the  $CB_2$  receptor space involved in the interaction with the examined molecules 1–20. In Figure 7 a new area with respect to Figure 3 of the

CB<sub>1</sub> model, region 8, appears in front of the aromatic ring of  $\Delta^9$ -THC. Carbons 11–13 of anandamide and its derivatives interact with region 8, and the resulting steric hindrance is negative for the binding. Similarly, a methyl substituent attached at the sp<sup>3</sup> carbon adjacent to the pyrroline ring nitrogen in **18** could be detrimental for binding. When compared with the analogous region in the CB<sub>1</sub> model (Figure 3), region 7 appears fractionated but extended closer to the phenolic OH of  $\Delta^9$ -THC. This OH group interacts with region 7, providing a negative contribution, and therefore, its removal would favor binding to the CB<sub>2</sub> receptor. This finding is consistent with literature data, demonstrating that the lack of the phenolic hydroxyl increases the selectivity toward the CB<sub>2</sub> receptor.<sup>41</sup>

Interactions with region 7 have a great impact on the CB<sub>2</sub> affinity of indoles **15**–**17** and of azoles **18** and **19**. The highly favorable interaction of morpholine methylenes with region 7 accounts both for the increased affinity of **15** with respect to the CB<sub>1</sub> receptor and for its CB<sub>2</sub> affinity, which is the highest among the indole analogues. Indoles **16** and **17**, exhibiting a C<sub>2</sub> indole methyl interacting with region 7, have appreciable CB<sub>2</sub> affinities, while **18** and **19**, where negligible interactions with region 7 exist, are of much lower affinity. Regions 3 and 4 of the CB<sub>1</sub> model merge in the CB<sub>2</sub> model (Figure 7).

Interaction of region 4 with the carbamido nitrogen of anandamides improves their binding affinities also in the CB<sub>2</sub> model, although the lack of the above interaction appears to be less relevant than in the CB<sub>1</sub> model. Table 1 shows a slightly lower CB<sub>2</sub> affinity of compounds **9** and **11** (having the amido nitrogen further away from region 4) with respect to anandamide **8**. The decreased affinity of compound **14** toward the CB<sub>2</sub> receptor is possibly due to the presence of an isopropyl group, which could interact with region 4, an interaction that could be associated with a decreased predicted affinity.

**Selectivity Model.** The correlation shown in Figure 5 and the high correlation coefficient demonstrate that the ligand affinity for the two receptors is very similar. To study selective regions for the interaction with CB<sub>1</sub> and CB<sub>2</sub> receptors, a specific methodology will be adopted. The method used is similar to that reported by Pastor et al.,<sup>42</sup> but in the present case the comparison is made between two ligand molecules rather than between two protein structures. Two compounds, one selective for the CB<sub>1</sub> receptor (anandamide derivative **10**) and the second for the CB<sub>2</sub> receptor (indole derivative **16**), were selected for comparison. The same superposition used in previous calculations was used as a reference.

Ten different GRID probes, reported in Table 3, were used in the GRID map calculation on both structures. The GRID maps were then unfolded in such a way that a 20-row matrix was obtained, 10 rows for the probe–**16** interactions and 10 for the probe–**10** ones.

PCA performed on the above matrix provided a two-component model explaining 90% of total variance. Figure 8 represents the score plot obtained from PCA. The horizontal axis discriminates between the two ligands, thus the first PC scores are proportional to the selective interactions of the two ligands with the dif-

**Table 3.** GRID Probes Used in the Selectivity Model

GRID probes <sup>a</sup>	symbol as in Figure 7	description
O	R2–C=O	sp <sup>2</sup> carbonyl oxygen
O–	Ar–O(–)	sp <sup>2</sup> phenolate oxygen
O=	R2–S=O	O of sulfate/sulfonamide
O::	RCOO(–)	sp <sup>2</sup> carboxy oxygen atom
OH	Ar–OH	sp <sup>2</sup> hydroxy group
O1	R–OH	sp <sup>3</sup> hydroxy group
N1:	NH(sp <sup>3</sup> )	sp <sup>3</sup> NH with lone pair
N1+	R3NH(+)	sp <sup>3</sup> amine NH cation
N3+	RNH3(+)	NH <sub>3</sub> <sup>+</sup> amine cation
DRY	DRY	hydrophobic probe

<sup>a</sup> Full probe details are defined in the GRID program.<sup>30,31</sup>

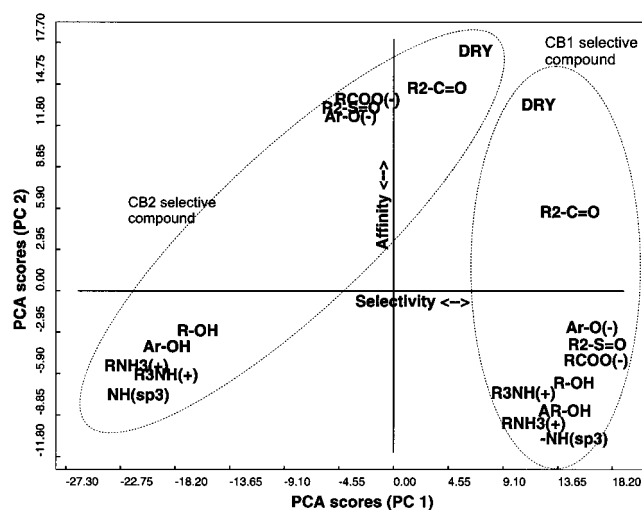


**Figure 8.** PCA score plot for the selectivity model. The first PC scores (*t*<sub>1</sub>) represent selectivity, while the second PC scores (*t*<sub>2</sub>) represent affinity. The GRID probes interacting with the two most selective compounds (anandamide derivative **10** and indole derivative **16**) belong to two separated ellipses.

ferent receptors. The vertical axis, discriminating between the different chemical probes, is proportional to the interaction power of each probe with respect to the two target structures. The latter differentiation is not interesting for our study and will be neglected in the present discussion.

When the probes are close in the score plot, their interactions are similar with both structures (see, for example, the hydrophobic probe DRY or the carbonyl oxygen O). These probes are not able to differentiate between the two selective ligands **10** and **16**, which probably do not interact with these residues in the receptors. On the contrary, when the probes are distant in the PC space, they are able to differentiate between the target molecules (see, for example, the charged H donor probe NH<sub>3</sub><sup>+</sup> or H donor probes such as R–OH and Ar–OH). As a consequence, amino acids such as Arg, Lys, His, Tyr, and Ser can be postulated as those providing selective interactions. When the selective regions extracted from the chemometric analysis<sup>42</sup> are reported in the 3D space (see Figure 9), the identification of selective regions becomes clear. Figure 9 reports the selective regions highlighted by the nitrogen H donor that could be representative of an histidine moiety. In the CB<sub>2</sub> selective compounds only one region, located opposite to the carbonyl group, is found. In this region histidine would be able to interact, giving an H bond with the carbonyl oxygen. It is important to stress that this region, corresponding to region 7 in Figures 3



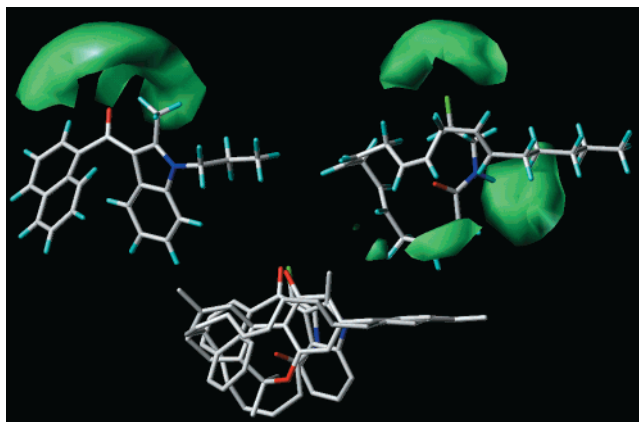


**Figure 9.** Selective regions evidenced by PCA analysis. The CB<sub>1</sub> selective compound (O585) is reported up-right and the CB<sub>2</sub> selective compound (JWH-015) up-left. Both selective compounds, superimposed to  $\Delta^9$ -THC chosen as template (H atoms are omitted for the sake of clarity), are reported below.

and 7, was found to be closer to the phenolic hydroxy group in the CB<sub>2</sub> model. However, the above region appears more clearly evidenced by this methodology, confirming its importance in modulating the selectivity toward CB<sub>2</sub>, as recently pointed out in the literature.<sup>41</sup> This region is less pronounced (and is weaker if the absolute values of the interaction energies are considered) in the CB<sub>1</sub> selective compound **10**, where a fluorine atom accepts the hydrogen of histidine. The geometry and the property of the accepting atoms in the two selective ligands make the difference in the interaction pattern.

The region opposite to the amidic NH of CB<sub>1</sub> selective compounds **10**, **13**, and **19** corresponds to region number 4 in the previous CB<sub>1</sub> receptor model. This region is not present at all in the CB<sub>2</sub> selective compound **16**. In this case an amino acid residue of the receptor is able to accept a hydrogen from the target NH. Visual inspection reveals another small region close to the carbonyl of the CB<sub>1</sub> selective compounds which is not present in the CB<sub>2</sub> selective compound. Again, the ligand carbonyl acts as H bond acceptor, but in this case it can accept only an H bond due to sterical hindrance. It is important to stress here that this region was not evidenced by the PLS model for the CB<sub>1</sub> receptor.

## Conclusions

The present work represents the first successful attempt to study by unique 3D-QSAR models the interactions of three structurally different classes of compounds with CB<sub>1</sub> and CB<sub>2</sub> receptors, respectively.

The high generality of the CB<sub>1</sub> and CB<sub>2</sub> PLS models is accompanied by a high statistical significance both in fitting and prediction achieved with only two PLS components. An independent procedure such as PCA, characterizing the compounds in order of binding affinity regardless of their structures, supported the selection of binding interaction regions.

A further PCA, using ten GRID probes, allowed us to compare quantitatively compounds selective for CB<sub>1</sub> and CB<sub>2</sub> receptors, respectively, as well as to identify the receptor selectivity regions. The CB<sub>2</sub> selectivity appears to be mainly due to the presence of a 3D interaction region located opposite to the carbonyl of the CB<sub>2</sub>

selective indole **16**, where an H-donor group of the receptor can interact with the ligand carbonyl. On the other hand, a region opposite to the amidic NH of the CB<sub>1</sub> selective anandamide **10** (where the receptor can accept H from the above NH) absent in the CB<sub>2</sub> selective compound appears to be responsible for the CB<sub>1</sub> selectivity.

**Acknowledgment.** We wish to thank MURST and CNR (Rome) for partial financial support of this work.

## References

- (1) Gaoni, Y.; Mechoulam, R. Isolation, structure and partial synthesis of an active constituent of hashish. *J. Am. Chem. Soc.* **1964**, *86*, 1646–1647.
- (2) Razdan, R. K. Structure-Activity Relationships in Cannabinoids. *Pharmacol. Rev.* **1986**, *38*, 75–149.
- (3) *Cannabinoids as Therapeutic Agents*; Mechoulam, R., Ed.; CRC Press: Boca Raton, FL, 1986.
- (4) Matsuda, S. A.; Lolait, S. J.; Brownstein, M. J.; Young, A.; Bonner, T. Structure of a cannabinoid receptor and functional expression of the cloned cDNA. *Nature* **1990**, *346*, 561–564.
- (5) Munro, S.; Thomas, K. L.; Abu-Shaar, M. Molecular characterization of a peripheral receptor for cannabinoids. *Nature* **1993**, *365*, 61–65.
- (6) Di Marzo, V.; De Petrocellis, L.; Bisogno, T.; Maurelli, S. Pharmacology and Physiology of the Endogenous Cannabinomimetic Mediator Anandamide. *J. Drug Dev. Clin. Pract.* **1995**, *7*, 199–219, and references therein.
- (7) Di Marzo, V.; De Petrocellis, L.; Bisogno, T.; Melk, D. Exogenous and endogenous cannabinomimetic metabolites. *Chim. Ind.* **1998**, *80*, 323–332, and references therein.
- (8) Devane, W. A.; Hanus, L.; Breuer, A.; Pertwee, R. G.; Stevenson, L. A.; Griffin, G.; Gibson, D.; Mandelbaum, A.; Etinger, A.; Mechoulam, R. Isolation and structure of a brain constituent that binds to the cannabinoid receptor. *Science* **1992**, *258*, 1946–1949.
- (9) Mechoulam, R.; Hanus, L.; Fride, E. Towards cannabinoid drugs-revisited. In *Progress in Medicinal Chemistry*; Ellis, G. P., Luscombe, D. K., Oxford, A. W., Eds.; Elsevier: Amsterdam, 1998; pp 199–243.
- (10) Reggio, P. H.; Seltzman, H. H.; Compton, D. R.; Prescott, W. R.; Martin, B. R. Investigation of the Role of The Phenolic Hydroxyl in Cannabinoid Activity. *Mol. Pharmacol.* **1990**, *38*, 854–862.
- (11) Little, P. J.; Compton, D. R.; Mechoulam, R.; Martin, B. R. Stereochemical effects of 11-OH- $\Delta^9$ -THC-dimethylheptyl in mice and dogs. *Pharmacol. Biochem. Behav.* **1989**, *32*, 661–666.
- (12) Mechoulam, R.; Devane, W. A.; Glaser, R. Cannabinoid geometry and biological activity. In *Marijuana/Cannabinoids Neurobiology and Neurophysiology*. Murphy, L., Bartke, A., Eds.; CRR Press: Boca Raton, FL, 1992; pp 1–33.
- (13) Reggio, P. H.; Greer, K. V.; Cox, S. M. The Importance of the Orientation of the C<sub>9</sub> Substituent to Cannabinoid Activity. *J. Med. Chem.* **1989**, *32*, 1630–1635.
- (14) Reggio, P. H.; Panu, A. M.; Miles, S. Characterization of a Region of Steric Interference at the Cannabinoid Receptor Using the Active Analogue Approach. *J. Med. Chem.* **1993**, *36*, 1761–1771.
- (15) Pinto, J. C.; Potie, F.; Rice, K. C.; Boring, D.; Johnson, M. R.; Evans, D. M.; Wilken, G. H.; Cantrell, C. H.; Howlett, A. C. Cannabinoid Receptor Binding and Agonist Activity of Amides and Esters of Arachidonic Acid. *Mol. Pharmacol.* **1994**, *46*, 516–522.
- (16) Adams, I. B.; Ryan, W.; Singer, M.; Thomas, B. F.; Compton, D. R.; Razdan, R. K.; Martin, B. R. Evaluation of Cannabinoid Receptor Binding and In Vivo-Activities for Anandamide Analogues. *J. Pharmacol. Exp. Ther.* **1995**, *273*, 1172–1181.
- (17) Adams, I. B.; Ryan, W.; Singer, M.; Razdan, R. K.; Compton, D. R.; Martin, B. R. Pharmacological and Behavioral Evaluation of Alkylated Anandamide Analogues. *Life Sci.* **1995**, *56*, 2041–2048.
- (18) Edgmond, W. S.; Campbell, W. B.; Hillard, C. J. The Binding of Novel Phenolic Derivatives of Anandamide to Brain Cannabinoid Receptors. *Prostaglandins, Leukotrienes Essent. Fatty Acids* **1995**, *52*, 83–86.
- (19) Thomas, B. F.; Adams, I. B.; Mascarella, S. W.; Martin, B. R.; Razdan, R. K. Structure-Activity Analysis of Anandamide Analogues: Relationship to a Cannabinoid Pharmacophore. *J. Med. Chem.* **1996**, *39*, 471–479.
- (20) Thomas, B. F.; Compton, D. R.; Martin, B. R.; Semus, S. F. Modeling the Cannabinoid Receptor: A Three-Dimensional Quantitative Structure-Activity Analysis. *Mol. Pharmacol.* **1991**, *40*, 656–665.

- (21) Tong, W.; Collantes, E. R.; Welsh, W. J.; Berglund, B. A.; Howlett, A. C. Derivation of a Pharmacophore Model for Anandamide Using Constrained Conformational Searching and Comparative Molecular Field Analysis. *J. Med. Chem.* **1998**, *41*, 4207–4215.
- (22) Schmetzer, S.; Greenidge, P.; Kovar, K. A.; Schulze-Alexandru, M.; Folkers, G. Structure–activity relationships of cannabinoids: A joint CoMFA and pseudoreceptor modelling study. *J. Comput.-Aided Mol. Des.* **1997**, *11*, 278–292.
- (23) Xie, X. Q.; Spiro, P.; DiMeglio, C. M.; Makriyannis, A. Conformational Studies on a Diastereoisomeric Pair of Tricyclic Nonclassical Cannabinoids by NMR Spectroscopy and Computer Molecular Modeling. *J. Med. Chem.* **1998**, *41*, 167–174.
- (24) Howlett, A. C.; Bidaut-Russell, M.; Devane, W. A.; Melvin, L. S.; Johnson, M. R.; Herkenham, M. The cannabinoid receptor: Biochemical, anatomical and behavioral characterization. *Trends Neurosci.* **1990**, *13*, 420–423.
- (25) Felder, C. C.; Veluz, J. S.; Williams, H. L.; Briley, E. M.; Matsuda, L. A. Cannabinoid agonists stimulate both receptor- and nonreceptor-mediated signal transduction pathways in cells transfected with and expressing cannabinoid receptor clones. *Mol. Pharmacol.* **1992**, *42*, 838–845.
- (26) Compton, D. R.; Rice, K. C.; De Costa, B. R.; Razdan, R. K.; Melvin, L. S.; Johnson, M. R.; Martin, B. R. Cannabinoid structure–activity relationships: Correlation of the receptor binding and in vivo activities. *J. Pharmacol. Exp. Ther.* **1993**, *265*, 218–226.
- (27) Showalter, V. M.; Compton, D. R.; Martin, B. R.; Abood, M. E. Evaluation of Binding in a Transfected Cell Line Expressing a Peripheral Cannabinoid Receptor (CB2): Identification of Cannabinoid Receptor Subtype Selective Ligands. *J. Pharmacol. Exp. Ther.* **1996**, *278*, 989–999.
- (28) SYBYL 6.4 Molecular Modeling Software, TRIPOS, Inc., 1699 S. Hanley Rd., St. Louis, MO, 1997.
- (29) Rosenqvist, E.; Ottersen, T. The Crystal and Molecular Structure of  $\Delta^9$ -Tetrahydrocannabinolic Acid B. *Acta Chem. Scand. B* **1975**, *29*, 379–384.
- (30) Goodford, P. J. A Computational Procedure for Determining Energetically Favourable Binding Sites on Biologically Important Macromolecules. *J. Med. Chem.* **1985**, *28*, 849–857.
- (31) Boobbyer, D. N. A.; Goodford, P. J.; Mcwhinnie, P. M.; Wade, R. C. New Hydrogen-Bond Potentials for Use in Determining Energetically Favourable Binding Sites on Molecules of Known Structure. *J. Med. Chem.* **1989**, *32*, 1083–1094.
- (32) Wade, R.; Clerk, K. J.; Goodford, P. J. Further development of hydrogen bond function for use in determining energetically favourable binding sites on molecules of known structure. Ligand probe groups with the ability to form two hydrogen bonds. *J. Med. Chem.* **1993**, *36*, 140–147.
- (33) Baroni, M.; Costantino, G.; Cruciani, G.; Riganelli, D.; Valigi, R.; Clementi, S. Generating Optimal Linear PLS Estimations (GOLPE): An Advanced Chemometric Tool for Handling 3D-QSAR Problems. *Quant. Struct.-Act. Relat.* **1993**, *12*, 9–20.
- (34) Pastor, M.; Cruciani, G.; Clementi, S. Smart region definition: A new way to improve the predictive ability and interpretability of three-dimensional quantitative structure–activity relationships. *J. Med. Chem.* **1997**, *40*, 1455–1464.
- (35) Cruciani, G.; Clementi, S.; Baroni, M. Variable selection in PLS analysis In *3D-QSAR in Drug Design, Theory Methods and Applications*; Kubinyi, H., Ed.; ESCOM: Leiden, 1993; pp 551–564.
- (36) Rich, M. R. Conformational Analysis of Arachidonic and Related Fatty Acids using Molecular Dynamics Simulations. *Biochim. Biophys. Acta* **1993**, *1178*, 87–96.
- (37) Corey, E. J.; Niwa, H.; Falck, J. R. Selective Epoxidation of Eicosa-cis-5,8,11,14-tetraenoic (Arachidonic) Acid and Eicosa-cis-8,11,14-trienoic Acid. *J. Am. Chem. Soc.* **1979**, *101*, 1586–1587.
- (38) Johnson, M. R.; Melvin, L. S. In *Cannabinoids as Therapeutic Agents*; Mechoulam, R., Ed.; CRC Press: Boca Raton, FL, 1986; pp 121–145.
- (39) Howlett, A. C.; Johnson, M. R.; Melvin, L. S.; Milne, G. M. Nonclassical Cannabinoid Analgesics Inhibit Adenylate Cyclase: Development of a Cannabinoid Receptor Model. *Mol. Pharmacol.* **1988**, *33*, 297–302.
- (40) Melvin, L. S.; Milne, G. M.; Johnson, M. R.; Subramaniam, B.; Wilken, G. H.; Howlett, A. C. Structure-Activity Relationships for Cannabinoid Receptor-Binding and Analgesic Activity: Studies of Bicyclic Cannabinoid Analogues. *Mol. Pharmacol.* **1993**, *44*, 1008–1015.
- (41) Huffman, J. W.; Yu, S.; Showalter, V.; Abood, M. E.; Wiley, J. L.; Compton, D. R.; Martin, R. B.; Bramblett, R. D.; Reggio, P. H. Synthesis and Pharmacology of a Very Potent Cannabinoid Lacking a Phenolic Hydroxyl with High Affinity for the CB2 Receptor. *J. Med. Chem.* **1996**, *39*, 3875–3877.
- (42) Pastor, M.; Cruciani, G. A Novel Strategy of Improving Ligand Selectivity in Receptor-Based Drug Design. *J. Med. Chem.* **1995**, *38*, 4637–4647.

JM991074S